

Illustrative Multivariate Visualization for Geological Modelling

A. Rocha¹, R. C. R. Mota¹, H. Hamdi², U. R. Alim¹, M. Costa Sousa¹

¹Department of Computer Science, University of Calgary, Canada

²Department of Geoscience, University of Calgary, Canada

Abstract

In this paper, we present a novel illustrative multivariate visualization for geological modelling to assist geologists and reservoir engineers in visualizing multivariate datasets in superimposed representations, in contrast to the single-attribute visualizations supported by commercial software. Our approach extends the use of decals from a single surface to 3D irregular grids, using the layering concept to represent multiple attributes. We also build upon prior work to augment the design and implementation of different geological attributes (namely, rock type, porosity, and permeability). More specifically, we propose a new sampling strategy to generate decals for porosity on the geological grid, a hybrid visualization for permeability which combines 2D decals and 3D ellipsoid glyphs, and a perceptually-based design that allows us to visualize additional attributes (e.g., oil saturation) while avoiding visual interference between layers. Furthermore, our visual design draws from traditional geological illustrations, facilitating the understanding and communication between interdisciplinary teams. An evaluation by domain experts highlights the potential of our approach for geological modelling and interpretation in this complex domain.

CCS Concepts

•**Visualization Application Domains** → Scientific Visualization; •**Physical Sciences and Engineering** → Earth and Atmospheric Sciences;

1 Introduction

Geological modelling involves incorporating various details (e.g., rocks and fluids) about the hydrocarbon-bearing formations into a discretized three-dimensional (3D) digital petrophysical model [RB15, HRBC14]. During the conception of these models, geologists and geophysicists conduct observations and experiments on datasets in different scales and modalities to create a reliable 3D representation. Since this process consists of information from several disciplines (i.e., geology, geophysics, petrophysics, reservoir engineering), it goes through several stages of data exploration (Figure 1 (a)). Common examples of observed datasets include seismic data and samples of rock information collected during the process of drilling known as coring [GA11]. In the domain, this model is known as a *geological model* or *static model* [GA11].

The geological models are represented regarding of meter-scale 3D cells known as *corner point cells*. These cells have irregular hexahedral geometry and are arranged along three dimensions (i , j , k) [Pon89] (Figure 1(b)). Since corner point grids are not required to be regularly spaced nor spatially continuous, they are suitable to encompass geological features such as horizons, fractures, dips, and faults, which are complex reservoir geometries challenging to model through conventional structured grids. At first, each cell is modelled to represent several *static* geological attributes such as rock type or facies. Later, this model is converted in a simulation model (generally a coarser version) where dynamic (time-varying) attributes are incorporated (Figure 1(a) (fifth stage)).

During geological modelling, geologists and reservoir engineers need to analyze several *geological properties* and *geological structures* to create a reliable version of a physical reservoir for optimal oil and gas recovery solutions. Despite their relevance, these are challenging, and time-consuming processes as current conventional geological modelling and visualization packages (e.g., Petrel® [Sch14] and CMG® [LTD14]) constrain users to visualize a single color-coded attribute at a time. This approach forces the user to frequently toggle between different attributes for supporting data exploration tasks. Moreover, the effort of keeping spatial reference between different regions of the data increases cognitive load since the user has to memorize each property individually and then perform the comparison [Sto06, LFK*13]. This representation also confounds the interpretation of geological scenarios since data semantics of the visual encoding are not accounted for. The complex geometry of these models makes the exploration of internal 3D geological structures even more difficult.

We present a novel illustrative multivariate visualization that addresses the aforementioned visualization challenges. We build upon Rocha *et al.*'s Decal-Maps [RASCS17] to augment the design and implementation of several geological attributes displayed on the surface layers of the geological models. The proposed method is accomplished by extending the Decal-Maps framework from a single surface to multiple (irregular) surfaces defined by the i , j and k directions of the corner point grid. This approach allows us to use the Decal-Maps technique in complex geological situations where multiple surfaces collapse, e.g., on regions containing faults or

pinch-outs, or when surfaces intersect each other, such as when grid aligned cross-sections are used to explore 3D internal structures—a common strategy adopted by reservoir engineers and geologists.

By combining colormaps, decals, decal-maps as well as a 3D glyph-based representation, we represent the following geological data attributes: *rock type* (categorical data), *porosity* (scalar data), *permeability* (tensor data), and *oil saturation* (scalar data). For porosity representation, we contribute a new importance-sampling strategy to generate decal distributions on the deformed corner point grid. For permeability, we propose a hybrid visualization strategy that combines 2D decals and 3D ellipsoid glyphs. Our perceptually-based design allows us to visualize additional geological attributes such as oil saturation, while avoiding visual interference between attribute layers. Our visual design draws from traditional geological illustrations, facilitating the understanding and communication between interdisciplinary teams. Moreover, we evaluate our technique with domain experts via real walk-through scenarios to highlight the potential of our approach for geological modelling and interpretation in this complex domain. Our main contributions in this work are as follows:

- A domain problem characterization to inform visualization practitioners new to the domain. We summarize the different data stages and task analysis encountered in this domain.
- A multivariate visualization design that allows us to visualize multiple geological attributes in a single view. By combining the concept of layering on surfaces, a 3D glyph-based representation and additional illustrative aspects, we create illustrative multivariate visualizations of geological models.
- An importance-based grid sampling method for producing density maps of scalar fields. We demonstrate its applicability for sampling porosity decals in geological models.
- An extension of the Decal-Maps technique to deal with complex geological situations. This extension further allows us to integrate the rendering of other objects into the layering pipeline.

2 Related Work

We focus on works that deal with the visualization and exploration of 3D geological reservoir models covering both techniques for visualizing multiple attributes as well as illustrative aspects.

2.1 Multivariate Visualization

Multivariate visualizations can support the process of data exploration by combining several attributes in one single view [FH09, KH13] and have also been applied to reservoir models. For example, Toledo and Celes [TC11] proposed a strategy to explore the visualization of multiple layers of multiphase (oil, gas, and water) reservoir simulation models by combining Line Integral Convolution (LIC) and colormaps. Höllt et al. [HdMRHH16] provide a system for visual analysis of reservoir simulation ensembles that combines color, which encodes the mean value of a given variable (e.g., water saturation), and a noise texture combined with blur, which indicates the uncertainty defined by the variance. Somanath et al. [SCSCS14] proposed an information visualization approach to explore well trajectories in post-simulation reservoir models that combines rock porosity and pressure to derive a new attribute that classifies the corner point cells into ‘fit’ (high porosity and high pressure) and ‘unfit’ (low porosity and low pressure) regions for the well trajectory. Compared to our approach, these works are ap-

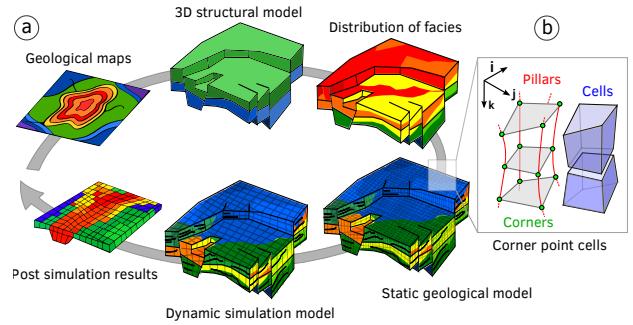


Figure 1: Illustrative scheme of the steps involved in creating a 3D geological model to be used in dynamic simulation.

plied to post-simulation models and dynamic attributes and are limited to representing one or two attributes at a time. Moreover, they do not take advantage of illustrative methods which are now well-established in the field [LVPI18].

Recently, Rocha et al. [RASC17] proposed Decal-Maps, a new approach to visualize multivariate data on arbitrary surfaces. By extending the concept of layering, the authors were able to design a multivariate geological visualization on the surface of a reservoir simulation model representing six attributes, namely *rock type*, *porosity*, and *oil and water flow rates*. This process was achieved by applying suitable design choices inspired by perception and traditional geological illustration. Our work is inspired by this previous work but differs from it in three main ways. (1) It extends the Decal-Maps technique to encompass geological scenarios and situations where surfaces intersect and collapse; this also allows us to integrate visual representations such as 3D glyphs into the layering pipeline. (2) It provides a design that is based on perceptual studies and traditional illustration. Our design improves the hybrid (2D and 3D) superimposed visualization of static geological attributes. (3) It presents a simple and efficient way to compute porosity distributions represented as decals on the geological surfaces.

2.2 Illustrative Techniques

Illustrative visualization [VSE*06, VI18] builds on the concept of visual abstraction that was born in traditional illustration and has been broadly applied in scientific visualization. Rautek et al. [RBGV08] categorize the abstraction paradigm into *low-level abstraction techniques*—techniques that seek to answer the question of *how* to visualize; and *high-level abstraction techniques*—techniques that focus on *what* to visualize and provide ways to explore the data based on the degree of interest.

For reservoir or geological models, there have been some efforts to provide visualizations and visual abstractions to improve data interpretation and understanding. Most of these techniques focus on *what* to visualize and aim to allow visual access to the internal parts of the 3D model. They are part of the *smart visibility* family of techniques that have mainly been applied to scientific data following the concept of importance driven visualization [Vio05]. Lidal et al. [LHV12] propose design principles for cutaway visualizations of geological models inspired by traditional geological illustration. Martins et al. [MFBCS*12] were the first to provide a cutaway approach for corner point grids to create a focus+context visualization of regions of interest. de Carvalho et al. [dCBM*16] extended this approach in terms of rendering and interactivity to create an inter-

active illustrative visualization of view dependent and independent cutaways. Techniques based on *exploded views* have also been proposed. Martins *et al.* [MFBCS15] applied exploded views to corner point grids using a BSP-tree approach. Sultanum *et al.* [SSSCS11] presented an approach of ‘splitting’ and ‘peeling’ to allow reservoir engineers to visualize the geological distribution of internal reservoir cells. Somanath *et al.* [SCSCS14] used transparency and an axis-aligned cross-section to visualize internal 3D well trajectories. In their approach, the corner point grid cells related to the well trajectory can also be displaced to the top of the reservoir model to improve visibility during the focus+context visualization.

On the other hand, very few works address *how* to visualize and are mostly applied to seismic data [PGTM07, PGT*08]. One exception is the work of Rocha *et al.* [RMC11] which provides a ray casting-based algorithm to apply line drawings to reservoir isosurfaces to highlight areas of high and low curvature. Here, we also focus on *how* to visualize and combine illustrative aspects such as line drawings with illustrative visual representations of geological attributes. Thanks to the concept of layering on surfaces and decals, our design allows us to visualize multiple attributes in a single view. It is by combining illustrative visual representations with illustrative rendering that we create illustrative multivariate visualizations of geological models.

3 Task Analysis and Goals

We now highlight some important workflows, task analysis and challenges in the oil and gas domain. For a broader domain problem characterization, we refer the reader to the supplementary material. Our characterization comes from our long-term collaboration with domain experts, literature review as well as previous studies conducted in this domain [SSSCS11, SCSCS14]. For our characterization, we use the *multi-level typology framework* [BM13]. This typology allows “the translation of empirically observable domain problems into abstract tasks and subsequently into design choices” [BM13]. For a given task, we identify *why* the task is performed, and discuss *how* the task will be supported. We explain *what* connects the input and output (if applicable) of a task. For more details, we refer the reader to [BM13, Mun14]. We use the labels **black** and **purple** bold to refer to **action** and **targets** under the *why* category, whereas **green** bold refers to the *how* category [Mun14].

3.1 Problem Characterization

In the oil and gas domain, static models are conventionally built to be input to flow simulators. These models need to capture the essential heterogeneity of properties (**trends**) that will impact reservoir simulation performance. Since the information from small scales (e.g., coring data and lab measurements) is interpolated/extrapolated to several meters following some geostatistical model [GA11], the amount of uncertainty that is introduced makes this task highly difficult. For this reason, geologists and geophysicists **explore** the **distribution** of these properties (within the reservoir model) to **verify** if the property modelling is appropriate or if it has spurious features (**outliers**) that do not agree with the well data. During these studies, they **explore** and **compare** geological attributes to **identify correlations** between properties and geological or petrophysical **trends** [RB15]. This task is even

more challenging since attributes have different data types (scalar, vector, and tensor) and semantics.

After the static model is built, reservoir engineers **explore** geological attributes as parameters for better prediction of oil recovery. They **identify** spatial configurations of static properties—e.g., **data correlations** and **geological features**—to **summarize** optimal reservoir development strategies and to better **predict** the dynamic reservoir performance before running costly fluid flow simulations. In particular, some efforts focus on combining static geological information to quantify reservoir connectivity, a **derived** property that has been shown to have a strong correlation with the efficiency of hydrocarbon recovery [HL10]. Connectivity is a necessary condition for reservoir productivity. For the assessment of optimal well placements, static connectivity analysis is used by engineers to **identify** multiple production scenarios, **locate** promising candidates, and further **pinpoint** the most promising scenarios for simulation.

Despite the aid of automated tools, the process of **locating** optimal placement scenarios for recovery still remains heavily exploratory and relies on the analysis and interpretation skills of a series of specialists who are the true driving force behind geological modelling and well optimization. Group work and analysis are also common for improving awareness of the data and reaching better decision making. Teams of engineers, geologists, geophysicists, and potentially other specialists may **summarize** recovery strategies; **summarize** the results from flow simulations; **identify** inconsistencies or interdependencies in the data; and finally, **present** optimal strategies to project managers and stakeholders.

3.2 Abstract Tasks

In this paper, we focus on the following tasks:

T1: The user can *discover* geological scenarios by *exploring* and *comparing* areas of high and low magnitude, and/or strong and weak directionality.

Why? **discover** → **explore** → **compare**

How? **Encode + Arrange + Change + Navigate**

T2: The user can *discover* geological scenarios by *exploring* geological distributions to *identify* correlations between static properties through *comparison*.

Why? **discover** → **explore** → **identify** → **compare**

How? **Encode + Arrange + Change + Navigate + Superimpose**

T3: The user can *discover* potential geological scenarios by *exploring* the distribution of geological properties to *identify* connected regions.

Why? **discover** → **explore** → **identify**

How? **Encode + Arrange + Change + Navigate + Filter + Superimpose**

T4: The user can *verify* possibilities for flow behavior by *exploring* the distribution of geological properties to *identify* correlations between static and dynamic properties (behavior).

Why? **verify** → **explore** → **identify** → **compare**

How? **Encode + Arrange + Change + Navigate + Superimpose**

T5: The user *presents* the results by *looking up* geological properties and summarizing the trends.

Why? **present** → **lookup** → **summarize**

How? **Encode + Arrange + Change + Navigate**

3.3 Design Goals

The following design goals draw from the previous abstract tasks to forge effective visualizations.

DG1: *Suitable representation of geological attributes.* Conventional software systems in this domain do not consider data types and data semantics. Our goal is to represent the static geological attributes (rock type, porosity, permeability and oil saturation) considering suitably designed visual encodings based on each data type. We anticipate that this greatly facilitates the understanding and interpretation of geological properties.

DG2: *Facilitate communication between multidisciplinary teams.* The oil and gas domain requires the communication between experts with different backgrounds for decision making. This aspect is a difficult task as the level of understanding of the scenarios varies according to the expertise. Details, for example, are not of interest to managers as reported in the study conducted by Sultanum et al. [SSSCS11]: “(Managers) don’t care about (cell-specific values), they just want to know ‘where is the oil’, ‘what is it doing there’, ‘what’s it gonna cost us to get it out’ (...)”. Creating illustrative visualizations that allow for an effective communication between people who are not familiar with the details of the domain would facilitate the understanding of the phenomenon.

DG3: *Facilitate the visualization of trends.* Based on our characterization, we observe that the target **trends** appears in several scenarios. This aspect is also verified in the study conducted by Sultanum et al. [SSSCS11] where many participants among 12 experts highlighted the importance of trends during exploration: “I am looking through specific trends and not through one specific value”. Similar comments also appeared in Cabral R. Mota et al.’s studies [MCS*16], where users highlighted the need to visualize the general trend of connected regions.

DG4: *Display of multiple attributes.* Users search for **correlations** in the data to confirm or discard hypotheses about flow behavior and geological scenarios. Due to the multivariate nature of geological models, this is a common scenario during geological modelling and flow prediction: “(...) it’s now showing porosity, and at the same time you want other property also displayed...” [SSSCS11]. However, as discussed previously, this mapping is usually limited to a single geological property [SCSCS14].

DG5: *Access the 3D nature of geological models.* Connected areas in geological models may go through several layers and may consist of several tortuous connected channels defined by the reservoir heterogeneity and geological structures. Therefore, developing methods for accessing such features is desired. Cross-sections and other methods (transparency) are commonly used by geologists and reservoir engineers even though several works have provided more sophisticated approaches [SSSCS11, SCSCS14, MFBCS15, dCBM*16, MCS*16].

4 Visualization Design

Guided by our design goals, in this section we explain **how** our visualization is designed to address the tasks presented in Section 3.2.

To begin with, we focus on the visual design of geological attributes (**DG1**). We draw inspiration from design aspects rooted in the fields of perception and information visualization [War12] (e.g., pre-attentive processing, color perception, and visual variables) as



Figure 2: Pastel colormaps (from ColorBrewer [BH]).

well as traditional illustration. These aspects allow us to encode data semantics and create visual metaphors. We believe they can improve the communicative power of our visualizations (**DG2**).

Our approach also builds upon the visual design of geological and fluid flow attributes introduced by Rocha et al. [RASCS17] and makes use of the concept of layering to visualize multiple attributes on the surfaces defined by the corner point grids of the geological model (**DG4**). Here, we present the design of the static attributes *rock type*, *porosity*, *permeability* and *oil saturation*. Our design is motivated by the fact that these static geological properties are the ones frequently examined in the domain workflow. Moreover, our design focuses on minimizing the interference between multiple layered attributes (**DG4**).

4.1 Static Geological Attributes

4.1.1 Rock Type

Rock type is categorical data represented as a set of indices. In geological models, generally 2–4 rock types are available. Categorical attributes covering large areas are better **encoded** using pastel colormaps, as done in 2D maps [War12]. Moreover, light tones are more suitable for background layers in the layering process [KML99, RASCS17, RSACS17]. In our approach, we only avoid the pastel blue tone since, based on our feedback from domain experts, it resembles water (saturation). Figure 2 illustrates the colormaps considered in our design.

4.1.2 Porosity

Porosity is a volumetric value expressed as a percentage that measures the capacity of rocks to store fluids [TD12]. Mathematically, it describes the fraction of void space in the material. It is defined by the ratio: $\phi = \frac{V_v}{V_t}$, where V_v is the volume of void-space and V_t is the total volume of the material.

Rocha et al. [RASCS17] presented an illustrative representation for porosity, which is intuitive to understand even without considering any domain background. This representation resembles stippling [MARI17] and builds on the porosity definition by using the metaphor of *clustered grains* of rock to **encode** porosity. In this representation, the *grains* are represented as *decals*, and the variation of porosity on the reservoir is **encoded** by **arranging** decals on the surface using a sampling strategy based on Poisson sampling [CCS12, YGW*15]. It provides a good strategy to convey **trends** of the porosity distribution in a smooth way, i.e., there is a smooth transition across cell boundaries. However, this approach has two disadvantages. First, importance Poisson sampling is an expensive sampling technique for arbitrary meshes; considering the context of corner point grids (where several types of degenerate cells are present) and the high resolution of geological models, this becomes even more expensive. Second, it does not provide fine control (cell or region based) of the porosity distribution; we cannot guarantee that the void space between the decals corresponds to the ratio of porosity. To address these issues, we propose a new importance sampling strategy for porosity (or any other scalar field).

Sampling. We refer the reader to Figure 3 to illustrate the discussion that follows. In our approach, we consider a sampling strategy *per cell face* of the reservoir grid. One could represent porosity

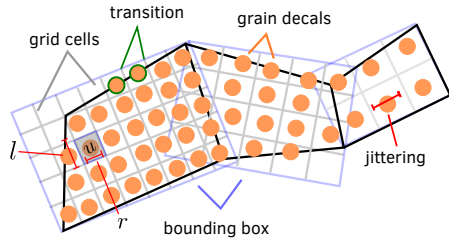


Figure 3: Porosity sampling illustration using our strategy.

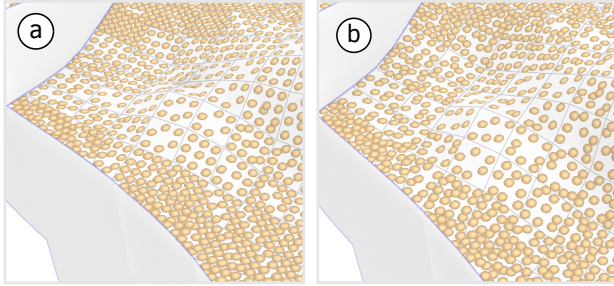


Figure 4: Porosity distribution on the surface of a geological model using our sampling approach. (a) No jittering; (b) jittering of 0.2.

within the entire cell using spheres as *grains*; however, we argue that this causes perceptual ambiguities due to projection (spheres equally spaced in 3D overlap in image space).

For our sampling, we first compute the planar bounding box that contains the face. We then subdivide this bounding box into a regular grid of square cells, where each cell u of the grid has side length l . Now consider a grain decal of radius r (radius of the sphere masking [RASCS17]) placed at the center of a cell u . Since porosity measures void space, for zero porosity we have the relationship that the area of the cell should be equal to the area of the decal, i.e., $\frac{l^2}{\pi r^2} = 1$, which means that the cell is 100% occupied. For a cell with 80% of the area occupied, the porosity is 0.2. Following this rationale, the length of cell u for a given porosity value p is given by the function $l_u(p) := r\sqrt{\pi(1-p)}$, where $0 \leq p \leq 1$ and r is the fixed radius of the decal. In geological models (sandstone reservoirs), values of porosity are usually between 0 and 0.4, therefore in the previous equation p never reaches 1. Next, we retain only the decals that fall on the face. In this approach, the total amount of void space given a porosity value p is simply the ratio of the sum of the areas of all grain decals and the area of the face; the resolution of the face grid and hence the number of grain decals is controlled by $l_u(p)$.

Figure 4 illustrates the grain decals placed after the sampling. To remove the grid pattern (if desired), we use a *stratified jittering sampling* strategy to jitter the decals around their centers (0.1–0.2 of r) slightly to make the distribution more uniform while preserving the porosity approximation. Our design also needs to consider that the faces may not be co-planar since each corner is independent (Figure 1). To address this issue, we modify our strategy to consider each triangle of the face. After the jittering process, for the generated triangle samples, we remove the ones at the common boundary that violate a defined minimal distance d (in our case $d = r$).

Discussion. It is important to highlight that our sampling approach is simple, approximates porosity and can be computed per face in

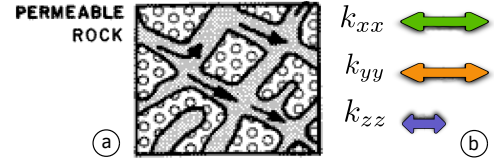


Figure 5: (a) Permeability illustration. (b) Permeability decals.

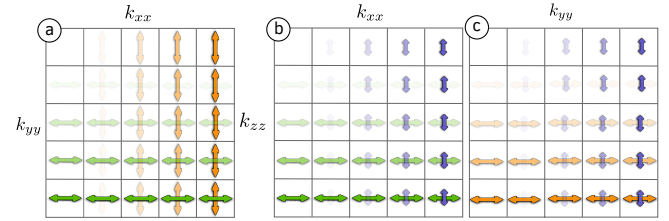


Figure 6: Permeability as 2D decal-maps.

parallel. One may argue that it can introduce bias and discontinuities at cell boundaries. However, thanks to the Decal-Maps approach [RASCS17], this problem does not arise as the decals always conform to the surface. Even if a decal is placed close to the boundary of a face, it will be mapped to the neighboring cell(s) *avoiding texture discontinuities*. In our tests, we did not observe any obvious bias in the porosity distribution (trends) (Figure 4(b)). Lastly, this approach can also represent other density attributes.

4.1.3 Permeability

Rock permeability is a tensor that indicates the ability of a medium to support fluid flow. Due to measurement limitations, geologists and reservoir engineers represent permeability as a diagonal 3×3 matrix to emphasize three predominant directions i , j and k in a curvilinear coordinate system. These directions have the permeability values k_{xx} , k_{yy} , and k_{zz} , respectively (i.e., the eigenvalues). If one considers the directions independently, the overall directionality is lost. Reservoir engineers analyze the magnitude of each component of this tensor to find potentially connected areas. Due to gravitational effects, the magnitude variation in sandstone reservoirs satisfies $k_{xx} \simeq k_{yy} \gg k_{zz}$.

Even though permeability is a tensor (i.e., tensor visualization has been proposed both in 3D [ROP11, BKC*13] and on surfaces [MVB*17]), to the best of our knowledge, it has only been represented using (rainbow) colormaps. This aspect makes the interpretation very cumbersome (hindering DG1, DG2, DG3 and even DG4) since the directionality is not encoded and the magnitude of the components can have different ranges. Therefore, here we present two new approaches to represent permeability.

Decal-based Representation. In geological illustration, permeability is depicted using arrows through a porous medium (Figure 5). Using this metaphor, we create *2D decal-maps* to **encode** permeability directions and their magnitudes (DG1, DG2, DG3). Since permeability is a symmetric quantity, in our visual encoding, we consider *double-sided arrows* to avoid bias. Due to their visual quality, we use Rocha *et al.*'s decal arrows [RASCS17] as a basis to create our permeability decals. We further assign a color to indicate each permeability direction. We choose orange, green and purple tones which offer a good contrast with the base layers (rock type and porosity) (DG4). Moreover, this approach allows us to (1) focus on a particular direction (selecting the category by

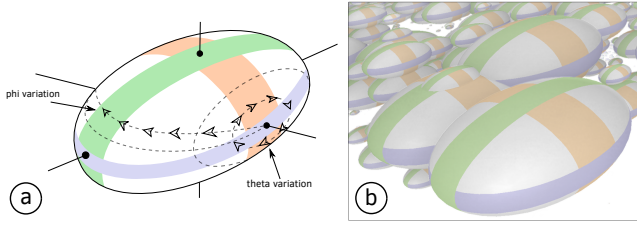


Figure 7: Permeability as 3D tensor glyph. (a) Orientation schematics; (b) design representation.

color) to check the magnitude variation (DG1) and (2) on the overall directionality (crossing double-sided arrows) to identify trends (DG1, DG2). Furthermore, to **encode** the magnitude of each direction, we **change** the transparency of the permeability decals. Since k_{zz} is much smaller than k_{xx} and k_{yy} , we also **change** the size of the permeability k_{zz} decals. This design comes from discussions with experts, who emphasized that when visualizing the permeability magnitude using colormaps, the normalization factor (normalize the scalar to map from 0 to 1) is misleading, since the strength of k_{zz} (represented as color) seems to be at the same scale of magnitude of k_{xx} and k_{yy} , but in reality, is much smaller. Last, we **arrange** the permeability decals at the center of each cell face. Figure 6 summarizes our decal-based representation.

Glyph-based Representation. To complement our decal-based representation on the reservoir surface, we also consider **encoding** permeability using 3D glyphs. One of the motivations is to augment the 3D exploration of connected areas of the reservoir (DG5). After some design interactions, we decided to **encode** permeability using *ellipsoid glyphs*. The reason for not using superquadric glyphs [Kin04] is that in reservoir engineering, the different shapes of the superquadric glyphs may be mistaken for different rock types. It is well-known that ellipsoidal glyphs have a problem of visual ambiguity; glyphs with differing tensor shapes exhibit similar image-space shapes [Kin04]. To solve the ambiguity problem, we propose a new approach for 3D glyph visualization.

Following a design point of view, we observe that the polar parametrization that defines an ellipsoid before deformation by the tensor eigenvalues can be used to highlight the glyph orientation during visualization (Figure 7(a)). In our case, the three orientations are aligned with the grid (i, j, k) directions. Therefore, by restricting ϕ and θ intervals and applying axis aligned 3D rotations, different visual representations can be designed. We **change** the 3D glyphs to **encode** the category colors of each permeability direction. For a given vertex v of the glyph, we obtain the angles θ and ϕ as $\theta = \tan^{-1}(v_y/v_x)$ and $\phi = \cos^{-1}(v_z/\rho)$, where $\rho = (v_x^2 + v_y^2 + v_z^2)^{\frac{1}{2}}$. Therefore, our (ϕ, θ) intervals are defined as $\epsilon + \frac{\pi}{3} \leq \phi \leq \frac{2\pi}{3} - \epsilon$, $\epsilon + \frac{4\pi}{3} \leq \phi \leq \frac{5\pi}{3} - \epsilon$ and $0 \leq \theta \leq 2\pi$. These intervals determine a *stripe* on the spherical surface whose thickness is controlled by the parameter ϵ (in our case $\epsilon = 0.3$). Stripes in the other directions are simply obtained by applying axial rotations to the vertex v . We color these stripes (lighter tone) with the permeability color related to the corresponding direction (category) and compose it with the color of the 3D tensor glyph (which in our case is light gray) that can also be used to **encode** another related quantity (e.g., transmissibility). This representation creates a correspondence between the 3D glyphs and the surface permeability decals. To place the glyphs

in 3D, we **arrange** the ellipsoid at the centroid of each cell. Each stripe reinforces the shape of the ellipsoid (e.g., being thinner when k_{zz} is small). We also **derive** the average magnitude from the three eigenvalues according to $k_{avg} = (k_{xx}^2 + k_{yy}^2 + k_{zz}^2)^{\frac{1}{2}}$. We then use this value to **change** the size of the 3D glyph. This helps decrease clutter by **filtering** areas of low magnitude and emphasizing areas of high permeability in 3D (DG5). Finally, the shape is deformed based on the diagonal scaling matrix $\frac{1}{k_{xx} + k_{yy} + k_{zz}}(k_{xx}, k_{yy}, k_{zz})$. Figure 7(b) illustrates our permeability 3D glyph representation.

4.1.4 Oil Saturation

Oil saturation is defined as the fraction of porous rock that contains oil. In our design, we **encode** oil saturation in the base layer (rock type) using the visual variable *value*, by changing the brightness of the pastel tones to darker tones. By following design guidelines [War12], we use four ranges of gray to allow the user to discriminate between tones. This design allows us to visualize trends in oil saturation and rock types in the same context (DG4).

4.2 Additional Design Considerations

Layering. Superimposing information is one of the most effective but the most challenging way of comparing and correlating attributes [GAW*11, KCK17], thus constituting the reason why the *power of layering* has been broadly used in visualization [KH13, Mun14]. Our design choices for representing attributes address the inter-layer interference of the visual elements (DG4). We consider several visual cues that allow identifying each layer individually while decreasing the interference caused by surrounding distractors [HE12]. Visual variables such as color, size, transparency as well as depth cues such as halos and shadows are essential to successfully achieve this. We also employ *gestalt principles* [War12] to allow users to complete superimposed information.

Visual Elements and Interaction. Apart from the geological attributes, we consider other illustrative elements such as *contours* in our visualization. For example, we apply contours on the surface layer of interest (focus) as well as the reservoir boundaries (context). Lighting also conveys information about the surface geometry but needs to be used carefully during the layering process [War12]. As in [RSACS17], we clamp some ranges of lighting and use two light sources (one at the viewer position and another one on top of the reservoir) to create a toon-like or light shading for the surface. Based on our observations, ambient occlusion is a good shading candidate to convey the surface curvature as well as enhance visual perception of geological structures (DG5). Moreover, since decals follow the surface curvature, they can represent the surface. For interactions, we consider **navigation** elements such as zooming, panning, and rotation. We also employ a *details-on-demand* approach by showing the striped directions on the 3D permeability glyph in a close view and fading it out based on the zoom level. The user is also given the ability to select and vary each layer of interest for 3D data exploration (DG5).

5 Implementation

5.1 Layering on Multiple Surfaces

As previously mentioned, our application technique builds upon the Decal-Maps layering framework [RASC17]. As demonstrated by Rocha et al., this framework is suitable to visualize multiple attributes on a *single* surface. In this framework, a decal layer is

defined by three steps; (1) G-buffer: geometry buffer with surface attributes; (2) SM-buffer: sphere masking buffer that selects areas of the surface to apply the decals; and (3) decal mapping: the process of applying decals on the surface using a local parametrization.

The SM-buffer requires that the intersection between the sphere and the surface be a disk. However, in the case of surfaces that intersect each other, a sphere close to the intersecting surfaces would lead to two intersections for a single decal. This would generate ambiguities in the decal mapping stage (3). This case can also arise when multiple surfaces are very close to each other, which causes the sphere to ‘bleed’ through the layers. These are all-too-common cases in the context of geological modelling (e.g., cross-sections, grid cells, pinch-outs, and faults). In this section, we address these issues by extending the layering technique.

5.2 Integration with the Layering Pipeline

The Decal-Maps technique is built on the deferred rendering pipeline [SWH13] and computes texture coordinates only for visible decals. In this pipeline, after the process of layering, attributes are represented in image-space.

Now let us consider a scenario where other objects, such as 3D tensor glyphs, need to be integrated with one or more layers in a single visualization. This scenario is not possible in Rocha *et al.*'s approach [RASCS17] since the depth test between the computed layer and the scene cannot be adequately handled; a naïve approach would be to render the layer over or below the scene. Here, we propose a solution to these problems which allows us to integrate the layering pipeline with the rendering of other visual representations such as the 3D permeability glyphs. In what follows, we present an overview of our implementation pipeline and discuss how it addresses the highlighted issues.

5.3 Pipeline Overview

Our implementation is GPU-based and employs a multi-pass rendering approach using OpenGL and GLSL. We refer the reader to Figure 8 to illustrate the discussions that follow.

5.3.1 Decal-Maps Extension

In our pipeline, we render *one surface* at a time; each surface corresponds to a layer (i, j, k) of the geological grid which we term G-Layer. For each surface, we can visualize one or more *attribute layers* (A-Layer). In our visualization, each A-Layer (in image-space) corresponds to one geological attribute.

AL-Buffer. Firstly, each A-layer is designed and rendered using decal-maps (porosity, permeability) or colormaps (rock type, oil saturation) by using the layering framework (Figure 8 left-middle). Then, we render the A-Layers of a chosen surface (G-layer) to one of the 2D textures of a 2D layered framebuffer object (LFBO) (off-screen pass). Assigning A-Layers to the LFBO can be accomplished by directly assigning the G-Layer id to the built-in variable `gl_Layer` in the geometry shader [SWH13]. It also does not require the depth test since all the A-Layers are already images. Moreover, since the A-Layers have access to the G-Buffer, we also store the depth and normal information in multiple color attachments [SWH13]. We apply this process to each surface layer of interest. At the end of this procedure, we obtain the *attribute layer buffer* (AL-Buffer) from the LFBO, which is a 2D array of textures containing the view-dependent information about the attributes as

well as the geometry of the surface (Figure 8 middle-right). Moreover, these layers are independent; decals coming from different G-Layers, therefore, do not affect each other (Section 5.1).

Rendering Integration. Now we need to address the problem of *sorting* the G-layers stored in the AL-buffer according to the depth order of the surfaces in object-space (Figure 8, right); the depth order is ignored when each surface layer is rendered separately. To address this issue, we draw a screen-quad in another pass and import the AL-buffer as a 2D texture array in the fragment shader. By accessing the surface depth stored in each texture, we perform an *insertion sort* in the fragment shader and sort the fragments and their corresponding attributes (color, normals) from front-to-back. Insertion sort is simple and works well for a small number of fragments that are already close to being sorted; this is indeed the case for layers coming from a geological model.

Since we cannot use dynamic allocation in the fragment shader, we define an array with a maximum number of G-Layers that our implementation supports (which can be adjusted depending on the dataset and application). This array is then filled with the depth information coming from the layers in the AL-Buffer. For sorting, this approach has no performance penalty due to the maximum length of the array; the algorithm is also not required to traverse the entire array. Therefore, we can simply initialize the array with a high number (i.e., generally, the depth buffer is normalized) and stop iterating when this number is reached. We thus obtain a sorted list of fragments, which we blend in a front-to-back order in a manner similar to volume rendering (Figure 8, right).

This approach allows us to effortlessly integrate the rendering of other objects within the layering pipeline. We solely render the objects to a framebuffer and incorporate this layer in the sorting process. Objects such as decals which are occluded by a surface are not rendered even when transparency is enabled (e.g., a layer only containing decals). Finally, image filters such as screen space ambient occlusion (SSAO) and blur are applied during post-processing.

5.3.2 Geological Attributes

We now connect our visual design with the layering framework.

Rock Type and Oil Saturation. In our design, rock type and oil saturation are represented using a pastel colormap and value, respectively. To encode them, we modify each pastel color to darker tones which are modulated by oil saturation values. In our visualization, these attributes are used as *base layers* following the painting metaphor [KML99, RASCS17].

Porosity. To represent porosity, we use the importance sampling strategy introduced in Section 4.1.2. The sampling is computed in the CPU in a pre-processing step. We pass the samples to the layering pipeline and render each grain decal on the surface to represent the overall porosity distribution.

Permeability. For permeability, we proposed two visual encodings: decals and 3D glyphs. For the decal approach, we first create an array of 2D textures containing the 2D tensor glyph combinations based on the permeability magnitude values encoded as transparency. These textures are passed to the fragment shader during the decal mapping stage where permeability eigenvalues are used to select the corresponding permeability representation from the 2D decal-map. For the 3D tensor representation, we draw spheres at cell centroids of the corner point grid using *instance render-*

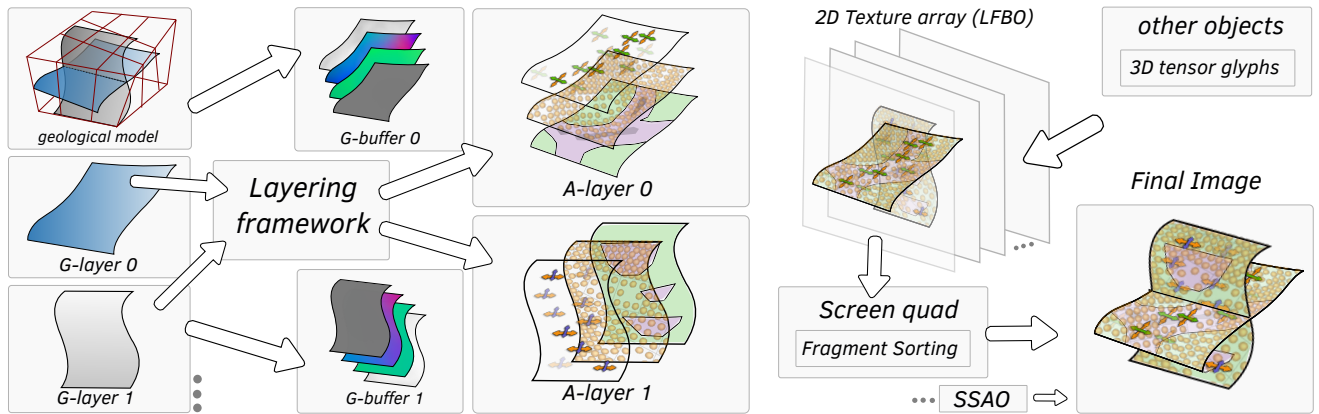


Figure 8: Implementation overview. (Left) Multiple layers are selected from the 3D geological model as input to the layering framework. (Middle) In the layering framework, attribute layers are computed and the G-buffer information (depth) stored in pixel-space. After this process, the layers are available in image space, but the depth relationship in object-space is lost. (Right) The A-Layers are rendered to a 2D texture array (layered framebuffer) and serve as input for a rendered screen quad in a subsequent pass. The layers are then sorted at the fragment level and the final image generated. After this process, filters such as SSAO can be applied.

ing [SWH13]. Then in the vertex shader, we apply the scale matrix defined by the permeability values to deform the vertices of the sphere glyph. Last, we render the stripes in the fragment shader and control their transparency based on the level of zoom.

5.4 Additional Illustrative Aspects

We also incorporate illustrative rendering aspects such as line drawings to improve the communication of our visualizations further [LVPI18]. When one layer of the model is being visualized (focus), it is essential to visualize the boundaries of the reservoir (context) to guide the user. For this, we render the outlines of the geological model and the outlines of the layers that are being visualized. We perform this in screen space by applying the Sobel edge detection filter to the depth buffer. Moreover, the grid of the geological model is visualized to help identify particular cells. To visualize the grid, we implement the single pass wire-frame approach [BNG*06] adapting the algorithm for quads and rendering it using light tones (to avoid visual interference). Moreover, to enhance the depth perception of our visualization, we also apply SSAO [Mit07] to the 3D permeability glyphs and the reservoir model. To improve SSAO quality and accuracy, we interpolate the normals of each layer. In our SSAO implementation, we consider 64 sample directions. Moreover, we also apply a Gaussian blur (5×5) to enhance rendering quality.

6 Results

In this section, we present results of our visual design and implementation. First through the lens of illustrative visualization followed by two case study scenarios used for a qualitative evaluation with a domain expert.

6.1 Illustrative Visualization

Our design considers several aspects of both perception and illustration. Based on our observations and domain expert feedback, these aspects improve the communication in the oil and gas domain (T5) as shown in our results. Figure 9(a) depicts our layering strategy where decals are placed on the reservoir surface for multiple properties (namely, permeability, porosity, and rock type). A layer with a fault reveals some interesting geological behaviors: moder-

ate vertical permeability, green-colored rock formations *pinching out* at the fault plane, and both porosity and horizontal permeability weakening as the distance from the fault increases. It is also worth noticing that our sampling strategy provides a smooth transition of porosity between grid cells, even adjacent to structural heterogeneities (e.g., faults and folds), and reservoir surface is shaded using a light intensity SSAO.

Figure 9(b) emphasizes the implementation of our visual encoding for the permeability tensor. There, the permeability tensor deforms the ellipsoids, and the average magnitude alters their size. Notice how the permeability is stronger in the i (k_{xx}) direction. The ellipsoid clusters also highlight—in 3D—the possible connected areas of the reservoir. In our design, we can further notice how the stripes created on the ellipsoid surface disambiguate the directionality of the tensor glyph. The stripes are also faded out based on the level of zoom as shown in the figure. Figure 9(b) also illustrates our hybrid visualization using decals, which is displayed in the cross-section (j) of the reservoir. There, we can obtain more details of the variability of the permeability on the surface in the j and k directions. Finally, the 3D tensor glyphs are shaded using SSAO, and edge detection filter is applied to highlight the contour of the surface and reservoir grid.

Finally, in Figure 9(c) we display an overview of our illustrative geological visualization (choosing different colors for the rock types). In this visualization, we can observe several geological scenarios such as faults and pinch-outs defined by the layers of the reservoir model. The ambient occlusion provides an excellent depth cue for discerning the inner part of the reservoir and the layered attributes. The overall rendition resembles traditional geological illustrations. We believe that the design concepts introduced in this paper and the results of their implementation significantly enhance the understanding of these complex models.

6.2 Expert Feedback

We present a qualitative evaluation with an expert reservoir engineer, a post-doctoral fellow with 7 years of academic experience and 4 years of industry experience. In close collaboration with our group, the expert advised us on domain-specific visualization chal-

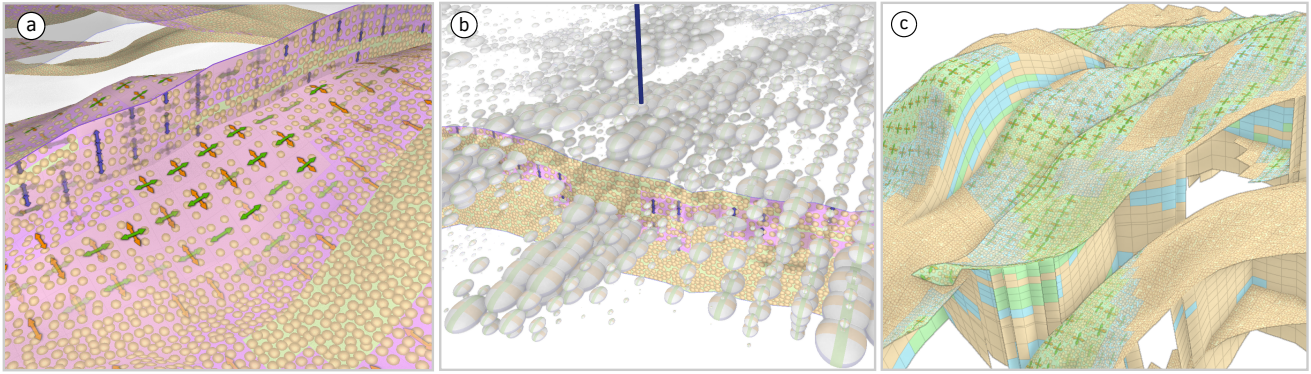


Figure 9: Illustrative multivariate geological visualization using our approach. (a) Two cross-sections depicting rock type, porosity, and the permeability tensor. (b) Hybrid visualization approach combining decals and 3D glyph tensor visualization. The 3D ellipsoid glyphs depict areas of high average permeability magnitude encoded by size. The glyphs shape illustrates the strong direction of permeability. (c) Illustrative geological visualization with an alternative design inspired by traditional geological illustrations [Bak16].

allenges and task requirements but was not involved in the design process. The purposes of this evaluation were to collect user's perceived usefulness and ease of understanding of our multivariate visualizations, as well as new design ideas for further refinements.

The evaluation session started with a description of motivations and goals of our work. Following this, the participant was introduced to two case study analyses. Each of these consisted of a brief introduction on how to interact with the system, executed by the researcher; and two semi-structured interviews. One addressed participant's subjective interpretation of the underlying case study, spurring them to identify problems, apply theory, and recommend courses of action. The second interview collected the participant's impressions on the usefulness, usability, as well as suggestions for improvements of our visual design.

The researcher adopted an inquiry-based learning approach throughout the session, guiding the participant by posing questions and relying on them to follow the assessment procedure and then communicating the findings. The participant was encouraged to interact with our visualizations and asked to think aloud to express reasoning.

6.2.1 Case Analysis I

Our first case analysis refers to a production scenario with secondary oil recovery, a hydrocarbon extraction method used to maintain reservoir pressure, while displacing oil towards the wellbore by injecting external fluid (e.g., water or gas). Figure 10(a) depicts the scenario; there is a pair of injecting (blue) and producing (red) wells connected through two sandstone channels.

Initial questioning spurred participant's interpretation of the underlying geology, such as "can you indicate regions with high permeability in the y-direction?" (T1) moreover, "can you identify areas with moderate porosity and oil saturation values?" (T2). From participant's quotes, it was observed that "one channel with isotropic homogeneous permeability behavior in x- and y- directions, and other [channel] with more accentuated permeability variability," and "both channels exhibit moderate porosity distribution; but different oil-saturation formations" (Figure 10(a)).

The following question was then posed to the participant. "For the case of water injection, what do you believe could happen and why?" (T4). "Given a reasonable distance between wells, and a

sufficiently large injection time", the specialist argued as plausible outcome that "water would start sweeping both channels but would be significantly faster in the straighter one (...) in a way that, at a certain time, fluid would be entirely displaced in this channel as the waterfront reaches the producing well. (...) and a small portion of the tortuous channel would be swept by the time water breaks through the producer" (T5).

Participant argued the answer was grounded on the diffusion coefficient, a parameter commonly used for proper characterization of mass transfer and its velocity during recovery processes. The diffusion process can be assumed as an expansion of a pressure head front (i.e., diffusion front), usually created at the wellbore whenever any changes (e.g., production or injection) happen.

For a single phase and slightly compressible fluid in an isotropic homogeneous medium, the diffusivity equation can be written as $\nabla^2 p = \frac{1}{\eta} \frac{\partial p}{\partial t}$, in which p is the fluid pressure, $\eta = k/(\phi\mu c_t)$ is the hydraulic diffusivity, k is permeability, ϕ is porosity, μ is viscosity, and c_t is the isothermal (t) compressibility factor. "Although the speed of single-phase pressure diffusion and saturation fronts are different, the effects of geological heterogeneities represent similar controls for the saturation front as in water flooding", the participant opined.

Diffusivity is thus a function of both fluid and medium properties, and the interplay between these significantly affects flow behavior and the likelihood of successfully waterflooding reservoir's reserves. In this sense, properties reflected in hydraulic conductivity would exert "predominant control, with water advancing in high permeability streaks, resulting in a breakthrough in the straight channel". As a side note, the participant mentioned structural aspects (e.g., sinuosity, layer thickness, or pinch-outs) can also be considered as resistance factors to the diffusive fluid transport in porous media.

Subsequent interviewing questions inquired: "is this a good or bad production forecast?" (T4); and despite answering to be not a bad outcome, the participant deliberated about drilling a new well in the unswept channel: "although permeability is not uniformly distributed here [the unflooded channel], there are small sandy bodies with accessible patches of oil (...) it makes sense to consider extracting oil using primary methods" (T5).

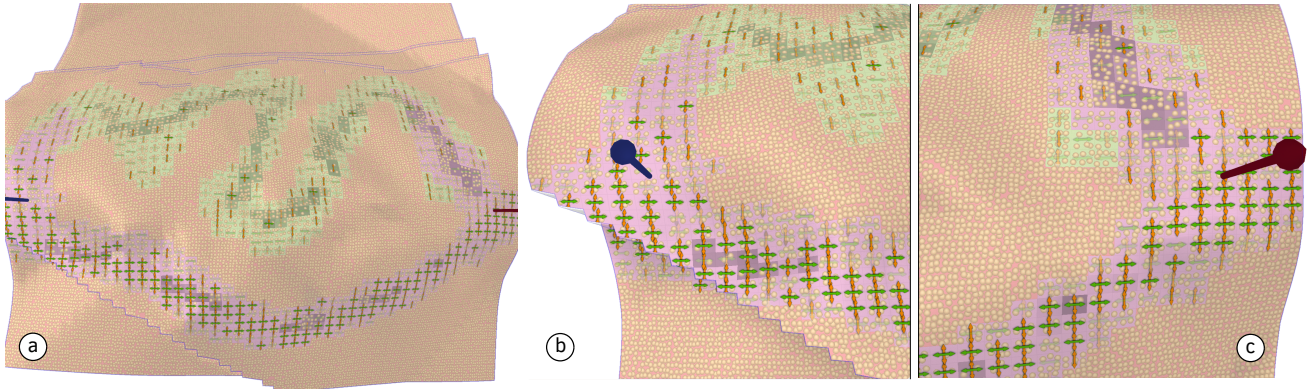


Figure 10: Illustrations of the secondary recovery analysis. At the reservoir surface, layered decals exhibit four properties that exert control over fluid behavior within the reservoir (namely, permeability, porosity, rock type, and oil saturation). From left to right: (a) top view of a geological model extracting oil using a pair of (b) injector and (c) producer wells.

When asked to compare our proposed multivariate visualizations (e.g., Figure 10(b) and (c)) with the current state of the art, the participant provided very positive comments—e.g., “*It is really good I can see everything at a glance. It is indeed multiple components and all of them impact the results (...) even considering just a few layers, I can see how my decision was quick; for the other one [Petrel software], the decision-making process would be lengthy as I would need to toggle between windows*”. We observed that the participant was most enthusiastic about the explicit encoding of permeability directions: “*This is really helpful. It is always confusing for me having to look at color bars for directional variables; and it can be problematic. Sometimes you see red grid blocks and mistakenly assume you have good connection in that area; but the strength is actually in only one direction and, maybe, zero in the other*”.

When prompted for ideas for improvements, the participant suggested a details-on-demand browsing model to inspect grid cells’ boundary and property distribution with high resolution and contrast. According to them, permeability decals are much useful for trend analysis. Nevertheless, given a high-resolution grid with sizable lateral variability, it could be challenging to diagnose structural and stratigraphic traps (e.g., pinch-outs and seals) as well as small cracks in rock permeability. Moreover, detecting these geological formations is essential for understanding oil and fluid capacities and flow behavior.

Also, despite recognizing it to be quite intuitive, the participant disapproved our design choice for oil saturation (with distinct HSV values). According to them, for scenarios with the presence of large oil pools, the readability of the underlying rock type would probably be harnessed. We observed this issue relates to the concept of integral-separable dimensions [War12]: interference occurs between data as color-value pairs tend to be perceived integrally but can be mitigated by using separable dimension pairs such as color-texture. The participant suggested a visual design for oil saturation that resembles the physical phenomena where, at the pore level, the oil *sticks* to rock formations; or a decal with combined porosity and saturation. We plan on investigating these ideas in the future.

6.2.2 Case Analysis II

The Second case analysis addresses inter-well connectivity and is illustrated in Figures 11 and 12, a production scenario based on an injector-producer well pair. As mentioned in Section 3, connec-

tivity is a fundamental condition for oil drainage. For successful secondary recovery particularly, both injecting and producing wells must be connected to generate sweep zones. Although multiple intertwined structural and stratigraphic properties can be considered for connectivity characterization, we here inspect the sand bodies. These are groups of neighboring cells with favorable permeability values, in which fluid flows at geologically reasonable rates.

Preliminary questioning encouraged the participant to inspect the dual permeability encoding (decal and tensor)—e.g., “*can you identify surface areas with low variability in horizontal permeability?*” (T1) and “*can you indicate internal regions with strong vertical permeability?*” (T1) (Figure 11(a)).

Following this, the participant was invited to interact with the visualization and asked: “*can you identify whether the two wells are connected?*” (T3). While switching between layers, the participant replied, “*from the 3D [tensors], I can see a stacked channel system that seems to extend across the two wells (...) the layers [decals] reinforce this, but I can also more easily compare permeability values in different directions*” (T5) (Figure 11(b)).

The composite visualization was well received; the participant praised once again the ability to inspect directional permeability—e.g., “*this is the right way of displaying permeability. (...) pressure drop exists in all three principal directions, and permeability can be measured for each of them*” and “*it is helpful especially for cases with severe anisotropy.*” The participant noted as a limitation, however, not being able to see decals due to occluding nearby tensors clearly; and suggested to either hide or reduce the visibility of those located in front of the decal layer (Figure 11(d)).

When questioned about the usefulness of our hybrid encoding strategy, the participant recognized it to be “*interesting complementary visualizations*”. According to them, tensors are most efficient for identification of patterns such as bulky sandy bodies and directional trends exhibited by permeability—“*it displays connectivity in 3D for the whole channeling system and provides better sense of connection compared to decals (...) whenever I spot an agglomerate [of tensors], it is intuitive to think of connected areas*”. In contrast, decals can be used for communicating heterogeneities at the cell level—“*it is easier to discriminate the magnitude of permeability in each direction*” (Figure 11(c)).

Beyond that, as decals can be quite valuable for comparing

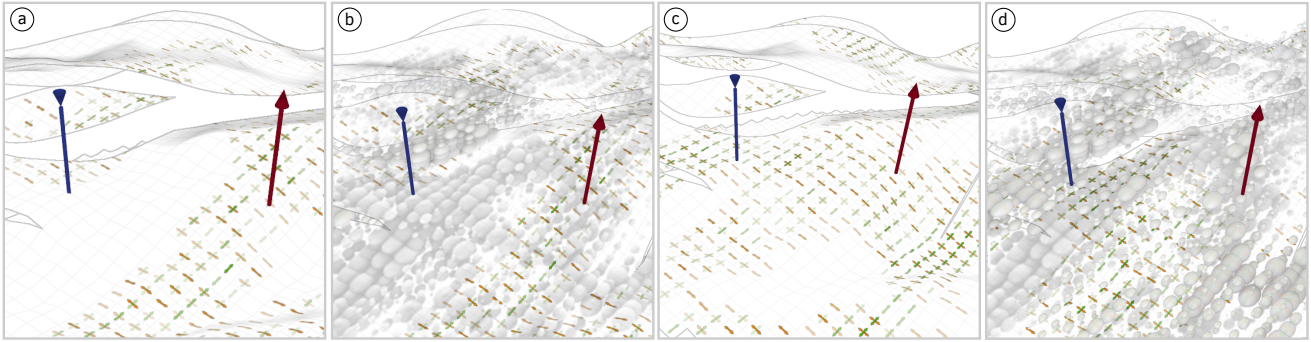


Figure 11: Illustrations of the inter-well connectivity analysis. (a) Permeability decals display no connection between wells at surface level. (b) 3D permeability tensors exhibit internal channeling networks. (c) Decals reveal interior inter-well connection in sandstone sheet. (d) Internal layer illustrating hybrid permeability encoding.

small-scale permeability fluctuations, the participant claimed the need for information on scale ranges. According to them, only considering transparency levels may lead to misleading judgments—“I see transparent decals, but how much impermeable are the [associated] cells compared to the most visible [opaque] ones?”. It is worth mentioning the loose decoupling from numerical data is intentionally enforced in our visuals, targeting two of our major design goals: quick sense-making (looking for patterns, trends, or exceptions) and ease of communication. However, providing quantitative estimates on demand (e.g., by clicking on decals) would be desirable in future refinements.

The participant claimed the added value of the tensor comes mostly from its shape, and thus suggested replacing its color-coded bands for additional attributes (e.g., 2- or 3-phase saturation decals, or transmissibility). In particular, encoding inter-cell transmissibility was said to be very convenient as “it tells me how easily ‘fluid moves’ between cells (...) is also directional, strongly dependent on permeability, and incorporates structural discontinuities across faces”. This is envisioned for future design iterations.

Another idea referred to the inclusion of fracture characterization illustrated as both decals and three-dimensional entities. As the participant argued, naturally occurring fractures have a significant effect on fluid flow in the form of increased permeability and permeability anisotropy. Hence, knowledge of the extent and orientation of fractures in relation to reservoir rocks helps engineers and geologists to optimize the well performance.

7 Conclusions and Future Work

We proposed a novel approach to create illustrative multivariate visualizations of geological reservoir models. We presented a problem characterization of the oil and gas domain as well as a set of abstract tasks obtained using the typology framework [BM13]. We selected a subset of these tasks that benefit from *multivariate visualization* and derived five design goals to guide our design and implementation. We also provided the first hybrid approach combining the concept of layering using decals and colormaps, a 3D-glyph based representation, and several illustrative aspects. This method was possible thanks to our implementation that addresses the problem of handling multiple surfaces and integrating different visualization pipelines with the layering framework. Our collaboration and evaluation by domain experts highlight the potential of our approach for geological modelling and interpretation. Our design

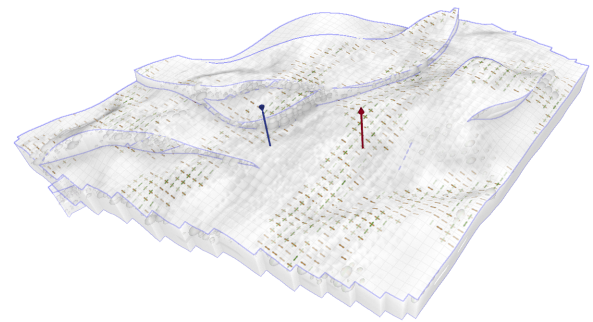


Figure 12: Geological model illustrating permeability as decal-tensor composition.

is grounded in domain knowledge and draws inspiration from perception and traditional illustration; we believe it has the potential to guide the multivariate visualization design in other domains. We acknowledge that by using the decal-based approach, one can design glyphs, marks and other visual representations to create metaphors that facilitate data understanding.

Since the design space is vast, we are curious to see which metaphors can be created for visualizing multivariate data in the future. As highlighted in our work, decals provide more detailed information whereas the 3D-glyph tensors provide an overview of the connected areas. Therefore, hybrid visualizations can also be an interesting research direction in the future for multivariate visualization. Moreover, our porosity density strategy can also be implemented in parallel and adapted to other density variables. Since reservoir models have many attributes (e.g., 20), even with excellent design choices, the visualization of multiple attributes in a single view is limited by our visual perception [War12]. Therefore, we draw inspiration from 2D abstract multivariate visualizations in InfoVis, and emphasize the need for new interaction techniques in SciVis that implement paradigms such as *details-on-demand* for managing multivariate data both on surfaces and in 3D, considering aspects such as temporal coherence, linked information and focus+context, which are essential to understand complex datasets.

Acknowledgments

We thank the anonymous reviewers for their constructive comments and feedback. This research was supported in part by the NSERC/AITF/FCMG Industry Research Chair Prog. in Scalable Reservoir Visualization and by Discovery Grants from NSERC.

References

- [Bak16] BAKEWELL R.: *An Introduction to Geology, Illustrative of the General Structure of the Earth: Comprising the Elements of the Science, and an Outline of the Geology and Mineral Geography of England*. Bibliolife DBA of Biblio Bazaar II LLC, 2016. Reprint (1813). 9
- [BH] BREWER C., HARROWER M.: Color brewer. URL: <http://colorbrewer2.org/>. 4
- [BKC*13] BORGIO R., KEHRER J., CHUNG D. H., MAGUIRE E., LARAMEE R. S., HAUSER H., WARD M., CHEN M.: Glyph-based visualization: Foundations, design guidelines, techniques and applications. *Eurographics State of the Art Reports* (2013), 39–63. doi:10.2312/conf/EG2013/stars/039-063. 5
- [BM13] BREHMER M., MUNZNER T.: A multi-level typology of abstract visualization tasks. *IEEE Transactions on Visualization and Computer Graphics* 19, 12 (2013), 2376–2385. doi:10.1109/TVCG.2013.124. 3, 11
- [BNG*06] BÆRENTZEN A., NIELSEN S. L., GJØL M., LARSEN B. D., CHRISTENSEN N. J.: Single-pass wireframe rendering. In *ACM SIGGRAPH 2006 Sketches* (2006), ACM, p. 149. doi:10.1145/1179849.1180035. 8
- [CCS12] CORSINI M., CIGNONI P., SCOPIGNO R.: Efficient and flexible sampling with blue noise properties of triangular meshes. *IEEE Transactions on Visualization and Computer Graphics* 18, 6 (2012), 914–924. doi:10.1109/TVCG.2012.34. 4
- [dCBM*16] DE CARVALHO F. M., BRAZIL E. V., MARROQUIM R. G., COSTA SOUSA M., OLIVEIRA A.: Interactive cutaways of oil reservoirs. *Graphical Models* 84, C (2016), 1–14. doi:10.1016/j.gmod.2016.02.001. 2, 4
- [FH09] FUCHS R., HAUSER H.: Visualization of multi-variate scientific data. *Computer Graphics Forum* 28, 6 (2009), 1670–1690. doi:10.1111/j.1467-8659.2009.01429.x. 2
- [GA11] GOMES J. S., ALVES F. B.: *The Universe of The Oil and Gas Industry*. Partex Oil and Gas, Lisbon, Portugal, 2011. 1, 3
- [GAW*11] GLEICHER M., ALBERS D., WALKER R., JUSUFI I., HANSEN C. D., ROBERTS J. C.: Visual comparison for information visualization. *Information Visualization* 10, 4 (2011), 289–309. doi:10.1177/1473871611416549. 6
- [HdMRHH16] HÖLLT T., DE MATOS RAVANELLI F. M., HADWIGER M., HOTEIT I.: Visual analysis of reservoir simulation ensembles. In *Proceedings of the Workshop on Visualisation in Environmental Sciences* (2016), Eurographics Association, pp. 1–5. doi:10.2312/envirvis.20161099. 2
- [HE12] HEALEY C. G., ENNS J. T.: Attention and visual memory in visualization and computer graphics. *IEEE Transactions on Visualization and Computer Graphics* 18, 7 (2012), 1170–1188. doi:10.1109/TVCG.2011.127. 6
- [HL10] HOVADIK J., LARUE D.: Stratigraphic and structural connectivity. *Geological Society, London, Special Publications* 347, 1 (2010), 219–242. doi:10.1144/SP347.13. 3
- [HRBC14] HAMDANI H., RUELLAND P., BERGEY P., CORBETT P. W.: Using geological well testing for improving the selection of appropriate reservoir models. *Petroleum Geoscience*, 4 (2014). doi:10.1144/petgeo2012-074. 1
- [KCK17] KIM K., CARLIS J. V., KEEFE D. F.: Comparison techniques utilized in spatial 3D and 4D data visualizations: A survey and future directions. *Computers & Graphics* 67, C (2017), 138–147. doi:10.1016/j.cag.2017.05.005. 6
- [KH13] KEHRER J., HAUSER H.: Visualization and visual analysis of multifaceted scientific data: A survey. *IEEE Transactions on Visualization and Computer Graphics* 19, 3 (2013), 495–513. doi:10.1109/TVCG.2012.110. 2, 6
- [Kin04] KINDLMANN G.: Superquadric tensor glyphs. In *IEEE TVCG/EG Symposium on Visualization 2004* (May 2004), pp. 147–154. doi:10.2312/VisSym/VisSym04/147-154. 6
- [KML99] KIRBY R. M., MARMANIS H., LAIDLAW D. H.: Visualizing multivalued data from 2D incompressible flows using concepts from painting. In *Proceedings of the Conference on Visualization* (1999), pp. 333–340. 4, 7
- [LFK*13] LIN S., FORTUNA J., KULKARNI C., STONE M., HEER J.: Selecting semantically-resonant colors for data visualization. *Computer Graphics Forum* 32 (2013), 401–410. doi:10.1111/cgf.12127. 1
- [LHV12] LIDAL E. M., HAUSER H., VIOLA I.: Design principles for cutaway visualization of geological models. In *Proceedings of Spring Conference on Computer Graphics (SCCG)* (2012), pp. 53–60. doi:10.1145/2448531.2448537. 2
- [LTD14] LTD. C. M. G.: Reservoir simulator software, 2014. URL: <http://www.cmg1.ca/software.1>
- [LVPI18] LAWONN K., VIOLA I., PREIM B., ISENBERG T.: A survey of surface-based illustrative rendering for visualization. *Computer Graphics Forum* 37 (2018). doi:10.1111/cgf.13322. 2, 8
- [MARI17] MARTÍN D., ARROYO G., RODRÍGUEZ A., ISENBERG T.: A survey of digital stippling. *Computers & Graphics* 67, C (2017), 24–44. doi:10.1016/j.cag.2017.05.001. 4
- [MCS*16] MOTA R. C. R., CARTWRIGHT S., SHARLIN E., HAMDANI H., COSTA SOUSA M., CHEN Z.: Exploring immersive interfaces for well placement optimization in reservoir models. In *Proceedings of the 2016 Symposium on Spatial User Interaction* (2016), ACM, pp. 121–130. doi:10.1145/2983310.2985762. 4
- [MFBCS*12] MARTINS FILHO Z., BRAZIL E. V., COSTA SOUSA M., DE CARVALHO F., MARROQUIM R.: Cutaway applied to corner point models. In *Workshop on Industry Applications (WGARI) in SIBGRAP I (25th Conference on Graphics, Patterns and Images)* (2012), pp. 7–12. 2
- [MFBCS15] MARTINS FILHO Z., BRAZIL E. V., COSTA SOUSA M.: Exploded view diagrams of 3D grids. In *28th Conference on Graphics, Patterns and Images (SIBGRAP I)* (2015), IEEE, pp. 242–249. doi:10.1109/SIBGRAP I.2015.12. 3, 4
- [Mit07] MITTRING M.: Finding next gen: Cryengine 2. In *ACM SIGGRAPH 2007 courses* (2007), ACM, pp. 97–121. doi:10.1145/1281500.1281671. 8
- [Mun14] MUNZNER T.: *Visualization Analysis and Design*. CRC Press, 2014. 3, 6
- [MVB*17] MEUSCHKE M., VOSS S., BEUING O., PREIM B., LAWONN K.: Glyph-based comparative stress tensor visualization in cerebral aneurysms. *Computer Graphics Forum* 36, 3 (2017), 99–108. doi:10.1111/cgf.13171. 5
- [PGT*08] PATEL D., GIERTSEN C., THURMOND J., GJELBERG J., GRÖLLER E.: The seismic analyzer: Interpreting and illustrating 2D seismic data. *IEEE Transactions on Visualization and Computer Graphics* 14, 6 (2008), 1571–1578. doi:10.1109/TVCG.2008.170. 3
- [PGTM07] PATEL D., GIERTSEN C., THURMOND J., MEISTER E. G.: Illustrative rendering of seismic data. In *Proceeding of Vision Modeling and Visualization* (2007), pp. 13–22. 3
- [Pon89] PONTING D. K.: Corner point geometry in reservoir simulation. In *ECMOR I-1st European Conference on the Mathematics of Oil Recovery* (1989). doi:10.3997/2214-4609.201411305. 1
- [RASCS17] ROCHA A., ALIM U., SILVA J. D., COSTA SOUSA M.: Decal-maps: Real-time layering of decals on surfaces for multivariate visualization. *IEEE Transactions on Visualization and Computer Graphics* 23, 1 (2017), 821–830. doi:10.1109/TVCG.2016.2598866. 1, 2, 4, 5, 6, 7
- [RB15] RINGROSE P., BENTLEY M.: *Reservoir model design*. Springer, 2015. 1, 3
- [RBGV08] RAUTEK P., BRUCKNER S., GRÖLLER E., VIOLA I.: Illustrative visualization: New technology or useless tautology? *SIGGRAPH Comput. Graph.* 42, 3 (Aug. 2008), 4:1–4:8. doi:10.1145/1408626.1408633. 2

- [RMC11] ROCHA A., MIRANDA F., CELES W.: Illustrative volume visualization for unstructured meshes based on photic extremum lines. In *24th SIBGRAPI Conference on Graphics, Patterns and Images (SIBGRAPI)* (Aug 2011), pp. 101–108. doi:10.1109/SIBGRAPI.2011.20.3
- [ROP11] ROPINSKI T., OELTZE S., PREIM B.: Survey of glyph-based visualization techniques for spatial multivariate medical data. *Computers & Graphics* 35, 2 (2011), 392–401. doi:10.1016/j.cag.2011.01.011.5
- [RSACS17] ROCHA A., SILVA J. D., ALIM U., COSTA SOUSA M.: Multivariate Visualization of Oceanography Data Using Decals. In *Workshop on Visualisation in Environmental Sciences (EnvirVis)* (2017), The Eurographics Association. doi:10.2312/envirvis.20171101.4,6
- [Sch14] SCHLUMBERGER: Petrel E&P software platform, 2014. URL: <https://www.software.slb.com/products/petrel>. 1
- [SCSCS14] SOMANATH S., CARPENDALE S., SHARLIN E., COSTA SOUSA M.: Information visualization techniques for exploring oil well trajectories in reservoir models. In *Proceedings of Graphics Interface 2014* (2014), Canadian Information Processing Society, pp. 145–150. doi:10.20380/GI2014.19.2,3,4
- [SSSCS11] SULTANUM N., SOMANATH S., SHARLIN E., COSTA SOUSA M.: Point it, split it, peel it, view it: Techniques for interactive reservoir visualization on tabletops. In *Proc. of the ACM International Conference on Interactive Tabletops and Surfaces (ITS)* (2011), ACM, pp. 192–201. doi:10.1145/2076354.2076390.3,4
- [Sto06] STONE M.: Choosing colors for data visualization. URL: https://www.cs.buap.mx/~dpinto/vi/choosing_colors.pdf. 1
- [SWH13] SELLERS G., WRIGHT R. S., HAEMEL N.: *OpenGL SuperBible: Comprehensive Tutorial and Reference*. Addison-Wesley, 2013. 7,8
- [TC11] TOLEDO T., CELES W.: Visualizing 3D flow of black-oil reservoir models on arbitrary surfaces using projected 2D line integral convolution. In *24th Conference on Graphics, Patterns and Images (SIBGRAPI)* (2011), IEEE, pp. 133–140. doi:10.1109/SIBGRAPI.2011.45.2
- [TD12] TIAB D., DONALDSON E.: *Petrophysics: Theory and Practice of Measuring Reservoir Rock and Fluid Transport Properties*. Gulf Professional, 2012. 4
- [VI18] VIOLA I., ISENBERG T.: Pondering the concept of abstraction in (illustrative) visualization. *IEEE Transactions on Visualization and Computer Graphics PP*, 99 (2018), 1–1. doi:10.1109/TVCG.2017.2747545.2
- [Vio05] VIOLA I.: *Importance-driven expressive visualization*. PhD thesis, Vienna University of Technology, 2005. 2
- [VSE*06] VIOLA I., SOUSA M. C., EBERT D., ANDREWS B., GOOCH B., TIETJEN C.: Illustrative Visualization for Medicine and Science. In *Eurographics 2006: Tutorials* (2006), The Eurographics Association. doi:10.2312/egt.20061068.2
- [War12] WARE C.: *Information visualization: perception for design*. Elsevier, 2012. 4,6,10,11
- [YGW*15] YAN D.-M., GUO J.-W., WANG B., ZHANG X.-P., WONKA P.: A survey of blue-noise sampling and its applications. *Journal of Computer Science and Technology* 30, 3 (2015), 439–452. doi:10.1007/s11390-015-1535-0.4